*CORROSION SCIENCE AND TECHNOLOGY, Vol.24, No.4(2025), pp.203~211* pISSN 1598-6462 / eISSN 2288-6524
[Research Paper] DOI: https://doi.org/10.14773/cst.2025.24.4.203

# Investigation into the Corrosion Mechanism of High-Voltage Cables in Eco-Friendly Vehicles

**Sungho Shin[1], Seungho Ahn[2], and Hyuntaeck Lim[1,†]**

*[1]R&D Strategy and Innovation center, Gwangju Institute of Science and Technology, Gwangju, 61005, Republic of Korea*
*[2]Electrification corrosion control research lab, Hyundai Motor Company, Hwaseong, 18280, Republic of Korea*
(Received July 17, 2025; Revised August 10, 2025; Accepted August 12, 2025)

This study investigates corrosion mechanisms in high-voltage (HV) cable connectors used in eco-friendly vehicles, focusing on galvanic and stray current corrosion under realistic operating conditions. Severe oxidation and pitting were observed at the interface between aluminum connectors and copper ground terminals, which are coated with tin (Sn). Mechanical fretting and electrical stress accelerated Sn layer breakdown, exposing the aluminum substrate and forming a galvanic couple with copper. A series of combined corrosion tests were carried out under vibration, DC bias, moisture ingress, and their simultaneous action. SEM/EDS analyses confirmed significant fretting wear and $Al_2O_3$ formation, especially when mechanical and electrical loads acted together. Leakage current measurements showed that both AC and DC systems produced current densities within critical stray current corrosion thresholds, particularly during deceleration and braking. These results reveal a synergistic degradation mechanism involving vibration, electrolyte exposure, and electrical bias. To mitigate corrosion, structural enhancements such as vibration-resistant fastening and environmental sealing are proposed. Overall, the findings provide new insight into HV connector failure mechanisms and present practical design recommendations to enhance durability and reliability in electric mobility applications.

***Keywords:*** *Corrosion, Eco-Friendly vehicle, High-Voltage cable, Corrosion mechanism, Surface characterization*

## 1. Introduction

The global transition toward eco-friendly transportation has accelerated the development and deployment of electric vehicles (EVs), hybrid electric vehicles (HEVs), and fuel cell electric vehicles (FCEVs) [1]. Driven by increasingly stringent environmental regulations, carbon neutrality targets, and advancements in battery and power electronics technologies, the market share of electrified vehicles continues to grow rapidly. These vehicles rely heavily on high-voltage systems (typically operating between 200–800 V) to efficiently transmit and control electrical energy between the battery, inverter, and traction motor. Among the various electrical components, high-voltage (HV) cables play a critical role in ensuring safe and stable energy transfer within the vehicle's powertrain and auxiliary systems [2]. HV cables must satisfy multiple functional requirements, including electrical insulation, thermal resistance, electromagnetic shielding, and mechanical durability under harsh automotive conditions such as vibration, moisture, temperature fluctuations, and chemical exposure. Depending on their function and current path, HV cables are typically categorized into single-phase direct current (DC) cables, which deliver power from the battery to the inverter or motor, and three-phase alternating current (AC) cables, which connect the inverter to the electric motor [3].

Despite their technical robustness, HV cables are susceptible to electrochemical degradation, especially at connector terminals and ground bonding points [4,5]. These regions often involve complex contact interfaces between dissimilar metals, and are subjected to cyclic mechanical stress, electrolyte exposure, and electrical bias, forming ideal conditions for corrosion initiation [6,7]. This corrosion not only compromises electrical performance and mechanical integrity but may also lead to thermal runaway, signal noise, or connector detachment, thereby threatening overall system reliability.

In general, automotive corrosion is understood to

†Corresponding author: htlim@gist.ac.kr
Sungho Shin: Researcher, Seungho Ahn: Research fellow, Hyuntaeck Lim: Professor

proceed via well-established mechanisms such as galvanic corrosion, pitting, and crevice corrosion, depending on material combinations and environmental factors. However, in the context of HV cable systems in electrified vehicles, several field and lab-based studies have reported non-conventional corrosion behaviors, including severe localized erosion, accelerated fretting, and early-stage failure unrelated to classic aluminum corrosion profiles [8,9]. For example, unlike conventional aluminum body corrosion, which typically proceeds via gradual oxide layer breakdown, excessive material loss and undercutting at the connector-ground interface have been observed in HV cable assemblies under simulated road salt and electrical loading conditions [10]. Such corrosion morphologies suggest the presence of synergistic degradation factors, including stray current corrosion, dissimilar metal contact with tin-plated components, and mechanical wear from vibration [11].

Galvanic corrosion is a form of electrochemical degradation that occurs when two dissimilar metals are electrically connected and simultaneously exposed to a corrosive electrolyte [12]. This phenomenon is driven by the potential difference between the two metals, causing one metal (the anode) to corrode preferentially while the other (the cathode) is protected. Especially, the severity of galvanic corrosion is directly related to the magnitude of the potential difference between metals, and it is generally considered significant when the difference exceeds approximately 0.25 V [13]. Furthermore, several factors such as higher ionic conductivity in the electrolyte and a low anode-to-cathode area ratio facilitate greater current flow, which directly enhancing corrosion kinetics. Stray current corrosion is an electrochemical phenomenon that occurs when unintended electrical currents, typically from external DC power sources, leak into conductive pathways such as metal structures or cable components [14]. These stray currents can enter a metallic conductor at one location and exit at another through a conductive electrolyte, leading to localized anodic dissolution and material degradation. Unlike galvanic corrosion, which depends on the potential difference between dissimilar metals, stray current corrosion is primarily governed by the presence of an external electrical field and the availability of an electrolyte that facilitates current leakage [15]. To evaluate the susceptibility of stray current corrosion, measurement of leakage current density is essential since it serves as a diagnostic indicator to identify potential corrosion risk zone.

Given these challenges, there is a clear need to systematically investigate the corrosion mechanisms specific to HV cable systems in eco-friendly vehicles. This study focuses on reproducing and analyzing failure scenarios observed in the field by combining material analysis (EDS/SEM), environmental simulation, and leakage current measurements under representative operating conditions. Through this investigation, the study aims to identify dominant degradation mechanisms and propose design or material countermeasures to improve the long-term durability of HV cable systems.

## 2. Experimental Methods

To investigate the corrosion mechanism of HV cables used in eco-friendly vehicles, two representative cable types were selected: a three-phase AC HV cable and a single-phase DC HV cable. The single-phase DC cable is responsible for delivering power from the HV battery to the motor drive unit, whereas three-phase AC cable transfers power from the vehicle's electric power control unit (EPCU) to the motor. As shown in Fig. 1, X-ray imaging reveals that both cable types for (a) AC and (b) DC, which share similar structural configurations and materials for the connector assembly and grounding interface. These components consist of the same housing shape and connection geometry, providing a consistent basis for comparative corrosion analysis. Preliminary observations under accelerated corrosion conditions using calcium chloride ($CaCl_2$) have shown that both cable types exhibit localized corrosion primarily at the lower section of the connector bracket, especially near the grounding junction area (highlighted in red dashed area in Fig. 1). This recurring pattern of severe material degradation across both cable types suggests a common corrosion pathway associated with the connector-ground interface.

To investigate this corrosion mechanism, detailed material characterization of the connector is essential since the initiation of corrosion was predominantly observed at the connector-ground interface. Note that the ground connection of the HV cables used in this study consists of a tinned copper (Sn-coated Cu) braided wire,

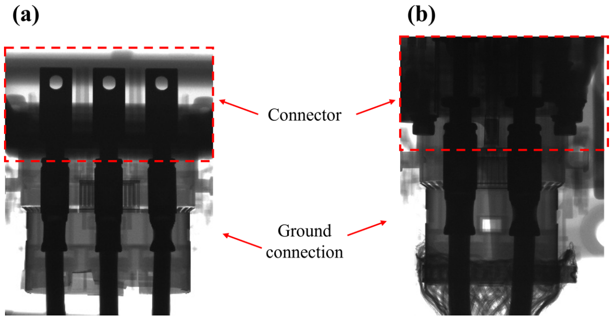


**Fig. 1. X-ray images of high-voltage cables: (a) AC cable, (b) DC cable**

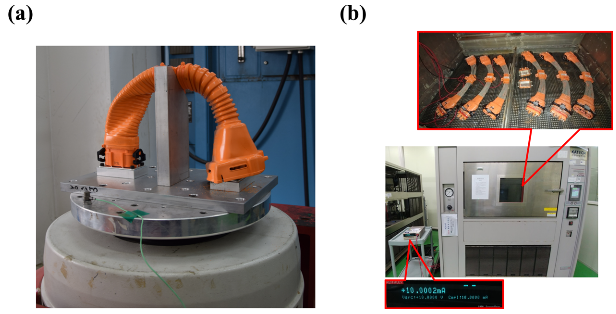


**Fig. 2. Failure-reproduction test setup: (a) vibration tester mounted specimen, (b) corrosion test chamber**

which plays a critical role in maintaining electrical continuity and shielding. Energy dispersive X-ray spectroscopy (EDS) was conducted on both the surface and cross-section of the connector region, and this analysis enabled the identification of material interfaces, coating integrity, and presence of corrosion products.

In parallel, to evaluate the susceptibility to stray current-induced corrosion, leakage current measurements were conducted using a high-sensitivity clamp-type meter under various simulated operating conditions. To simulate realistic conditions, the test environment was maintained at 35 ºC and 95 % relative humidity. Both AC and DC high voltage of around 400 V were applied to the HV cable specimens during leakage current measurements. The measurement scenarios included 1) Idle condition, 2) Forward and reverse rotation, 3) Forward braking, 4) Reverse braking of vehicle. These operational modes reflect typical drivetrain behaviors in eco-friendly vehicles, and were used to quantify electrical leakage across both AC and DC HV cable configurations.

Fig. 2 illustrates the experimental setups used for failure mechanism reproduction and principle validation for (a) a vibration endurance tester configured with the connector mounted in its actual vehicle position, and (b) a corrosion test chamber used for evaluating the effects of combined environmental stressors. To assess mechanical degradation due to vibration-induced damage during vehicle operation, random vibration endurance testing was conducted following ISO 16750-3 specifications [16]. This test simulates mechanical fatigue and defect risk (e.g., component detachment, cracking, wear etc.) caused by road-induced excitation. A total 24 hours of vibration testing was performed, with 8 hours of excitation applied along each axis (X, Y, and Z). To evaluate fretting wear

**Table 1. Experimental conditions and test plan for combined corrosion testing**

| No. | 1 | 2 | 3 | 4 |
|---|---|---|---|---|
| Power application | × | O | × | O |
| Salt spray exposure | O | O | O | O |
| High temperature and humidity | O | O | O | O |
| Connector mating (Dissimilar metal contact) | O | O | O | O |
| Vibration test | × | × | O | O |

at the connector interface resulting from vibration, both surface and cross-sectional analyses were carried out using Scanning Electron Microscopy (SEM) and EDS.

For comprehensive simulation of real-world degradation, a combined corrosion test was designed based on four test conditions, as detailed in Table 1. The objective was to validate the impact of realistic structural assembly and power supply configurations, and to determine potential failure mechanisms. In all test cases, a constant DC power of 10.0 mA (2.0 $mA/cm^2$) was applied to simulate operating conditions. Each corrosion test cycle consisted of salt spray exposure (3 hours at 35 ºC with 5% NaCl solution), and high temperature and humidity aging (14 hours at 49 ºC and 95% relative humidity). Upon completion of a total of 14 test cycles were conducted, SEM and EDS were also performed on the connector contact regions to investigate corrosion morphology and material transformation.

## 3. Results

### 3.1 Identification of potential corrosion mechanisms

Table 2 summarizes the EDS analysis results for

**Table 2. EDS results of target HV cable**

| Elements | Connector surface (wt%) | Connector cross-section (wt%) |
|---|---|---|
| O | 33.10 | - |
| Na | 0.83 | - |
| Al | 0.52 | 92.31 |
| Ni | - | 1.00 |
| Cl | 0.33 | - |
| Sn | 59.13 | - |

different regions of the HV cable connector. On the connector surface, the detected elements included oxygen (O), sodium (Na), aluminum (Al), chlorine (Cl), and tin (Sn, about 59.13 wt%). These results confirm the presence of a tin (Sn) plating layer on the connector surface, likely applied for corrosion protection and contact conductivity. In contrast, the connector cross-section revealed the following elemental composition such as aluminum (Al, about 92.31 wt%), and nickel (Ni). This indicates that the bulk material of the connector is primarily composed of aluminum, with possible Ni interlayer or diffusion barrier coating. Since the ground terminal section of the HV cable consists of copper (Cu) with a thin layer of tin coating, therefore, the connector and ground contact points are not dissimilar metals owing to Sn-coated under initial conditions. However, it was noted that if the tin coating on either surface wears off due to mechanical abrasion or vibration-induced fretting, the underlying Cu-Al may become exposed, forming a dissimilar metal junction and promoting galvanic corrosion.

The leakage current values obtained under various vehicle operating conditions are summarized in Table 3 for the AC HV cable, and in Table 4 for the DC HV cable. According to established literature and electrochemical corrosion models, stray current corrosion is likely to occur when the leakage current density within the following threshold ranges of about 3 ~ 80 mA/cm$^2$ for AC [17] and about 0.01 ~ 10 mA/cm$^2$ for DC [18], respectively. Notably, if the current density surpasses these ranges significantly, corrosion tends to decrease sharply due to the formation of protective oxide layers or passivation films on the metal surface. However, when values remain within the critical window, the system is highly vulnerable to active corrosion processes, especially in the presence of conductive electrolytes.

In this study, the measured current densities for both AC and DC HV cables during forward braking and reverse braking conditions fell within the critical range, indicating a high risk of stray current-induced corrosion under these operational states, as shown in both Table 3 and Table 4. Additionally, in the DC HV cable, minor corrosion risk was also observed under forward and reverse driving conditions as shown in Table 4, where the current densities were measured at 3.25 mA/cm$^2$ (AC measurement), and 0.09 mA/cm$^2$ (DC measurement). Overall, the results indicate that both AC and DC HV cables exhibit significant vulnerability to stray current corrosion during braking operations, regardless of the applied voltage type. This highlights the critical importance of insulating integrity, connector design, and current path control in HV systems for eco-friendly vehicles.

Fig. 3 presents the results of the fretting wear reproduction test conducted to simulate vibration-induced mechanical damage at the connector interface. Fig. 3a

**Table 3. Leakage current measurement in three-phase AC HV cable**

| Measurement condition | Contact area | Operating condition | Measured value (mA/cm$^2$) | Corrosion possibility |
|---|---|---|---|---|
| AC current | 5.90 cm$^2$ | Idle | 0.25 | No |
| | | Forward/Reverse rotation | 2.70 | No |
| | | Forward stop | 12.14 | Yes |
| | | Reverse stop | 4.26 | Yes |
| DC current | 5.90 cm$^2$ | Idle | 0.00005 | No |
| | | Forward/Reverse rotation | 0.01 | No |
| | | Forward stop | 0.06 | Yes |
| | | Reverse stop | 0.06 | Yes |

**Table 4. Leakage current measurement in single-phase DC HV cable**

| Measurement condition | Contact area | Operating condition | Measured value (mA/cm$^2$) | Corrosion possibility |
|---|---|---|---|---|
| AC current | 2.67 cm$^2$ | Idle | 1.73 | No |
| | | Forward/Reverse rotation | 3.25 | Yes |
| | | Forward stop | 40.93 | Yes |
| | | Reverse stop | 19.42 | Yes |
| DC current | 2.67 cm$^2$ | Idle | 0.0009 | No |
| | | Forward/Reverse rotation | 0.09 | Yes |
| | | Forward stop | 1.17 | Yes |
| | | Reverse stop | 0.90 | Yes |

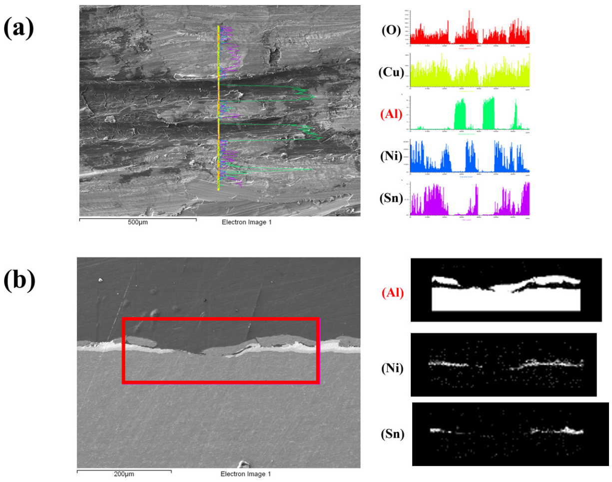


**Fig. 3. Wear test results: (a) surface, (b) cross-section**

shows SEM and EDS analyses of the worn surface, and Fig. 3b shows the corresponding cross-sectional SEM and EDS results. The surface EDS analysis as shown in Fig. 3a reveals a clear exposure of Al in the fretted region, indicating that the Sn plating layer has been worn off due to repeated mechanical contact. Similarly, as shown in Fig. 3b, cross-sectional EDS mapping within the red-line highlighted area also confirms localized exposure of the Al base material, verifying that the wear penetrated beyond the protective Sn coating. From three repeated test cycles, the average wear depth of the aluminum substrate was measured to be approximately 11.8 µm, indicating significant mechanical degradation of the connector material under vibration loading. These findings strongly suggest that vehicle-induced vibration during operation can lead to mechanical failure of the Sn coating, resulting in direct contact between the Al connector and Cu ground terminal. Such a dissimilar metal interface creates an ideal condition for galvanic corrosion, particularly in moist or conductive environments. As a result, progressive aluminum erosion and pitting corrosion may occur over time.

### 3.2 Results of combined corrosion testing

Fig. 4 through Fig. 7 present SEM and accompanying EDS results obtained from the connector surface after combined corrosion test conditions from 1 to 4 as listed in Table 1. For each specimen, three random sites were examined on both the left- and right-hand sides of the connector, such as Fig. 4a and Fig. 4b respectively, and the averaged elemental compositions (wt%) are summarized in Table 5. Under condition 1 as shown in Fig. 4, the connector surfaces showed no evidence of fretting or corrosion without electrical current and vibration operation. The major detected element was Sn, accounting for more than 75 wt%, with minor traces of Ni, likely from the under-plating layer beneath the Sn coating. It was indicated that the Sn layer remained fully intact and corrosion did not initiate under these inert conditions since Al and O were not detected on the surface. Similarly, where a 10 mA DC current was applied without vibration as shown in Fig. 5, the EDS results were similar to the result of condition 1. The absence of Al and O signals, along with the preservation of a high Sn content, indicated that electrical bias alone did not compromise the integrity of the protective coating or induce any measurable corrosion activity.

In contrast, Fig. 6 resulted in significant surface changes when vibration was operated to the HV cable. SEM images revealed localized wear regions with fretting damage, particularly in the red dashed zones as shown in both Fig. 6a and Fig. 6b. EDS spectra from these regions revealed the emergence of more than about 3 wt% of Al and increased O content, indicating that the Sn layer had been mechanically disrupted, ultimately exposing the underlying Al substrate. The presence of oxygen is attributed to the formation of $Al_2O_3$, a typical by-product of galvanic corrosion when Al is exposed to a conductive environment. Further degradation was observed under condition 4 as shown in Fig. 7, which combined mechanical vibration with DC electrical bias. In this case, the Al content increased by approximately 2 wt% relative to condition 3, while O content exhibited an increment

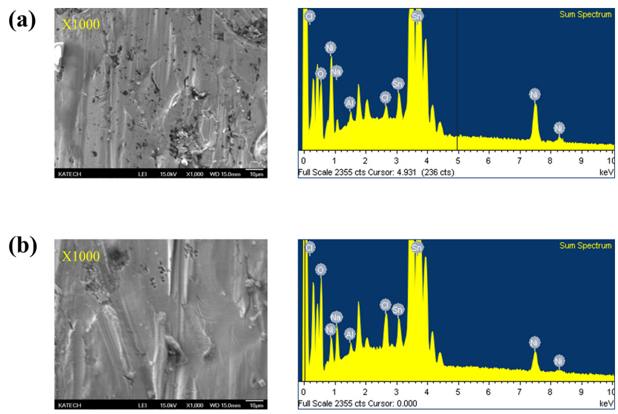

**Fig. 4. Combined corrosion test – condition 1: (a) left side, (b) right side**

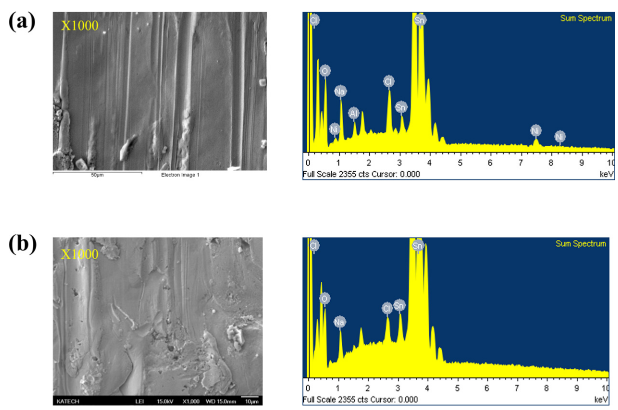

**Fig. 5. Combined corrosion test – condition 2: (a) left side, (b) right side**

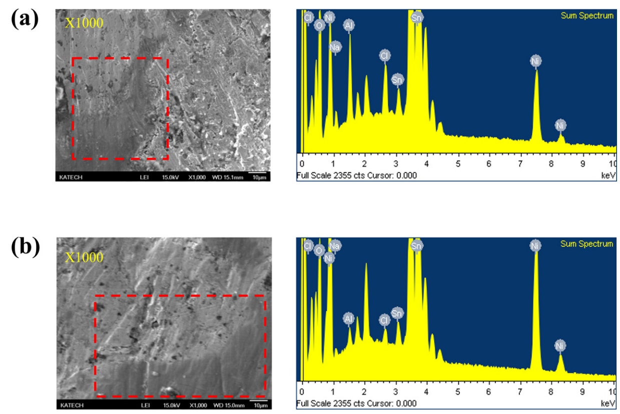

**Fig. 6. Combined corrosion test – condition 3: (a) left side, (b) right side**

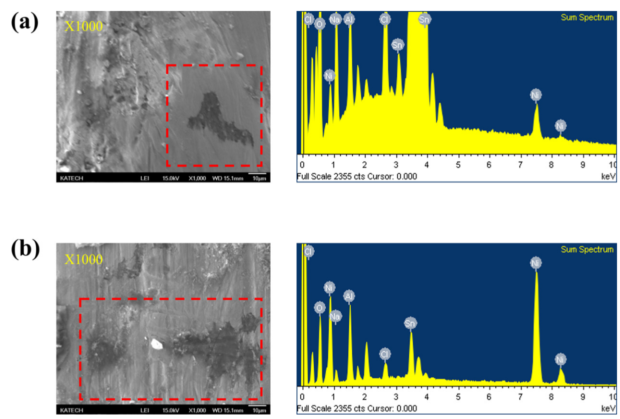

**Fig. 7. Combined corrosion test – condition 4: (a) left side, (b) right side**

**Table 5. Elemental analysis from combined corrosion test (Unit: wt%)**

| Elements | Condition 1 | Condition 2 | Condition 3 | Condition 4 |
|---|---|---|---|---|
| O | 11.30 | 16.68 | 17.87 | 26.62 |
| Na | 0.79 | 1.72 | 0.97 | 2.91 |
| Al | - | - | 3.11 | 5.35 |
| Ni | 9.22 | 3.94 | 10.84 | 3.56 |
| Cl | 0.39 | 1.01 | 1.60 | 5.44 |
| Sn | 77.94 | 76.65 | 75.61 | 56.12 |

exceeding about 10 wt%, suggesting that the presence of current accelerated oxide formation and substrate degradation. These findings point to a synergistic effect between mechanical abrasion and electrochemical activation, promoting both galvanic and stray current corrosion mechanisms.

These findings demonstrate that mechanical fretting is the primary initiator of coating failure, while concurrent DC bias amplifies corrosion kinetics once the Al-Cu dissimilar interface is exposed. Consequently, both galvanic and stray-current mechanisms act synergistically under realistic vehicle braking scenarios. Once exposed, the presence of electrical bias significantly amplifies corrosion kinetics, accelerating the deterioration process. These results emphasize the critical role of maintaining coating integrity and mitigating vibrational stress to prevent premature failure of HV connectors under realistic operating conditions.

## 4. Discussion

This study was initiated following repeated observations of severe corrosion and surface degradation at the connector–ground interface of high-voltage (HV) cables in eco-friendly vehicles. Field-returned connectors exhibited intensive oxidation and pitting, prompting a detailed investigation of the underlying mechanisms. Material analysis confirmed that the connector body is primarily Al, while the ground braid is Cu, with both surfaces plated with Sn for conductivity and corrosion protection. Evidence of dissimilar metal coupling suggested coating breakdown under service conditions.

Galvanic corrosion may arise when two dissimilar metals with significantly different electrochemical potentials are electrically connected and exposed to a conductive electrolyte. When the potential difference exceeds approximately 0.25 V, the less noble metal is prone to possibly accelerated anodic dissolution under typical service conditions such as measured in seawater [19]. In the present case, Al and Cu exhibit standard electrode potentials of approximately -0.75 V and -0.36 V, respectively, resulting in a potential difference of around 0.4 V. Although the aluminum-copper couple exhibits a significant difference in standard potential in this study, the actual galvanic behavior should be validated against measured corrosion potentials in the intended operating environment.

Furthermore, exposure of the connector region to electrolytic solutions such as road salt, rainwater, or condensation accelerates corrosion. Higher electrolyte conductivity and greater surface wetting increase the reaction rate. Without adequate sealing and structural countermeasures, HV cable systems become progressively more susceptible to electrochemical failure. To evaluate the corrosion mechanism under controlled yet representative conditions, four combined corrosion test scenarios were designed, varying vibration loading and electrical bias to isolate and assess the effects of mechanical wear (fretting) and stray current corrosion. Leakage current measurements during braking confirmed that stray current-induced electrochemical stress, combined with mechanical wear, accelerates degradation. The results clearly indicated that vibration-induced fretting is a key initiator of damage: repeated micro-motions mechanically remove the Sn coating, exposing the Al substrate. Once exposed, the Al contacts Cu directly, forming a galvanic couple. Compromised sealing permits electrolyte ingress, completing the corrosion circuit. Under these conditions, galvanic and stray current corrosion act simultaneously, producing high concentrations of $Al_2O_3$, as confirmed by EDS analysis.

Based on the elemental analysis in Table 5, the oxygen (O) content on the connector surface varied significantly depending on the test condition, ranging from 11.30 wt% to 26.62 wt%. Since elevated oxygen levels are indicative of aluminum oxide ($Al_2O_3$) formation, these results suggest that higher O content correlates with increased corrosion product accumulation. Comparing conditions 2 and 3, it is evident that vibration alone (condition 3) leads to a greater increase in O content than bias alone (condition 2), implying that mechanical fretting plays a more dominant role in initiating coating failure and subsequent corrosion. However, the highest O content was observed under condition 4, where both vibration and bias were applied simultaneously. This supports the hypothesis of a synergistic effect, whereby vibration-induced coating damage exposes the aluminum substrate, and the presence of stray current accelerates the electrochemical corrosion process once the dissimilar metal interface is exposed. Taken together, these findings confirm that the interplay between vibration, environmental exposure, and electrical current under realistic vehicle conditions creates a high-risk environment for accelerated corrosion. The degradation is not attributable to a single factor but rather to the synergistic effect of structural, material, and operational stressors.

Although noble metal coatings such as gold provide excellent corrosion resistance, conductivity, and environmental stability, their high cost and minimal thickness (typically 0.1–0.3 μm) limit their practicality [20]. Thin gold layers may also exhibit porosity and arc-tracking issues in high-current applications, making them unsuitable for cost-sensitive automotive systems.

Given these material limitations, structural reinforcement of the connector is proposed as a more practical and scalable solution. Specifically, mechanical designs that employ bolted or clamped retention can minimize micro-gaps at the contact interface and suppress relative movement that leads to fretting [21]. Increasing the contact normal force through latch redesign or spring preload can further enhance mechanical stability. In addition, sealing strategies such as precision-fitting connector tubes, dual O-ring configurations, and over-molded grommets can be employed to prevent moisture or electrolyte ingress [22]. For example, both main power and ground connection interfaces shall incorporate O-ring seals made of fluorocarbon material, compressed to 20-25% of their cross-sectional diameter within precision-machined grooves. By eliminating environmental triggers and maintaining mechanical tightness, the risks of galvanic and stray current corrosion can be greatly reduced. Additional measures, such as composite or duplex coatings (e.g., Sn–Ag, Sn–Bi), nanocrystalline Sn layers with enhanced wear resistance, and integrated leakage current sensing (e.g., Hall sensors), may further improve durability and enable early detection of insulation degradation.

Ultimately, this study demonstrates that while tin-coated connectors fulfill baseline performance and cost requirements, their durability can be compromised under real-world conditions involving vibration and electrical loading. A combined approach, involving mechanical design reinforcement, environmental sealing, and targeted material enhancements, offers a promising path forward for improving the long-term reliability of high-voltage connectors in eco-friendly vehicle platforms.

## 5. Conclusions

This study systematically elucidated the corrosion mechanisms affecting high-voltage cable connectors in eco-friendly vehicles, emphasizing the interplay between galvanic coupling and stray current-induced degradation. Material characterization and environmental testing confirmed that vibration-induced fretting is the primary trigger for protective layer failure, exposing the aluminum substrate to corrosive environments. Under simulated vehicle conditions, including thermal humidity, salt spray, and electrical bias, aluminum oxide formation was consistently observed, indicating active corrosion. Leakage current measurements under representative driving scenarios revealed that both AC and DC HV cables operate within the critical range for stray current corrosion, particularly during braking. The oxygen content analysis further showed that vibration had a greater impact on corrosion initiation than electrical bias alone, while the combination of both factors resulted in the highest corrosion product formation, demonstrating a clear synergistic effect.

These findings highlight the necessity of mitigating vibration-induced mechanical wear and controlling stray current pathways. Structural improvements such as vibration-resistant fastening, equivalent sealing of both power and ground connections, and prevention of electrolyte ingress are essential to enhance the long-term reliability and operational safety of HV cable systems in electric mobility applications.

## References

1. A. Tafida, W. S. Alaloul, N. A. B. W. Zawawi, M. A. Musarat, and A. S. Abubakar, A Review of Eco-Friendly Road Infrastructure Innovations for Sustainable Transportation, *Infrastructures*, **9**, 216 (2024). Doi: https://doi.org/10.3390/infrastructures9120216
2. M. Bukya and R. Kumar, *Proc. PARC Conf.*, p. 485, IEEE, Mathura, India (2020). Doi: https://doi.org/10.1109/PARC49193.2020.236661
3. G. E. Sfakianakis, J. Everts, and E. A. Lomonova, *Proc. EVER Conf.*, p. 1, IEEE, Monte Carlo, Monaco (2015). Doi: https://doi.org/10.1109/EVER.2015.7112939
4. M. Jarvid, M. H. Larsen, K. M. Bengtsson, and S. Hansson, *Proc. ICHVE Conf.*, p. 1, IEEE, Berlin, Germany (2024).

Doi: https://doi.org/10.1109/ICHVE61955.2024.10676232

5. H. Y. Lee, S. H. Ahn, and H. T. Im, A Research on Stray-Current Corrosion Mechanism of High Voltage Cable Connector on Electrification Vehicles, *Corrosion Science and Technology*, **18**, 117 (2019). Doi: https://doi.org/10.14773/CST.2019.18.4.117
6. Y. R. Yoo, D. H. Kim, G. B. Kim, S. Y. Won, S. H. Choi, and Y. S. Kim, Galvanic Corrosion Between Component Parts of Aluminum Alloys for Heat Exchanger of Automobile, *Corrosion Science and Technology*, **22**, 322 (2023). Doi: https://doi.org/10.14773/cst.2023.22.5.322
7. S. Y. Hur, J. M. Jeon, K. T. Kim, and Y. S. Kim, Control of Galvanic Corrosion Between A516Gr.55 Steel and AA7075T6 Depending on NaCl Concentration and Solution Temperature, *Corrosion Science and Technology*, **19**s, 281 (2020). Doi: https://doi.org/10.14773/cst.2020.19.6.281
8. A. Rafati, H. Mirshekali, H. R. Shaker, and N. Bayati, Power Grid Renovation: A Comprehensive Review of Technical Challenges and Innovations for Medium Voltage Cable Replacement, *Smart Cities*, **7**, 3727 (2024). Doi: https://doi.org/10.3390/smartcities7060144
9. J. Su, B. Du, J. Li, and Z. Li, Electrical tree degradation in high-voltage cable insulation: progress and challenges, *High Voltage*, **5**, 353 (2020). Doi: https://doi.org/10.1049/hve.2020.0009
10. J.-M. Lim, B.-S. Kim, S.-H. Ahn, and J.-G. Kim, Galvanic Corrosion of Tinned Copper Coupled with Aluminum Alloy in Electric Vehicle, *Corrosion*, **80**, 746 (2024). Doi: https://doi.org/10.5006/4478
11. Z. Chen, D. Koleva, and K. van Breugel, A review on stray current-induced steel corrosion in infrastructure, *Corrosion Reviews*, **35**, 397 (2017). Doi: https://doi.org/10.1515/corrrev-2017-0009
12. S. Shukrey, S. Yenugu, S. Shah, and R. Bernardi, Corrosion Prediction Model for Electrical Components in Automobiles, SAE International, Warrendale, PA, SAE Technical Paper 2024-26–0307 (2024). Doi: https://doi.org/10.4271/2024-26-0307
13. F. Mansfeld, D. H. Hengstenberg, and J. V. Kenkel, Galvanic Corrosion of Al Alloys I. Effect of Dissimilar Metal, *Corrosion*, **30**, 343 (1974). Doi: https://doi.org/10.5006/0010-9312-30.10.343
14. J.-M. Lim, E.-H. Park, Y.-W. Kim, B.-S. Kim, S.-H. Ahn, and J.-G. Kim, Effect of Current Flow on the Galvanic Corrosion in Electrical Parts of Electric Vehicles, *IEEE Transactions on Transportation Electrification*, **11**, 1324 (2025). Doi: https://doi.org/10.1109/TTE.2024.3404033
15. C. Wang, S. Chowdhury, and X. Liang, Transmission Structure Corrosion Due to Stray Currents and the Inspection and Mitigation Techniques: A Review, *IEEE Transactions on Industry Applications*, **60**, 4677 (2024). Doi: https://doi.org/10.1109/TIA.2024.3362920
16. C.-J. Kim, Accelerated Sine-on-Random Vibration Test Method of Ground Vehicle Components over Conventional Single Mode Excitation, *Applied Sciences*, **7**, 805 (2017). Doi: https://doi.org/10.3390/app7080805
17. S. Goidanich, L. Lazzari, and M. Ormellese, AC corrosion. Part 2: Parameters influencing corrosion rate, *Corrosion Science*, **52**, 916 (2010). Doi: https://doi.org/10.1016/j.corsci.2009.11.012
18. C. Yang, G. Cui, Z. Li, Y. Zhao, and C. Zhang, Study the Influence of DC Stray Current on the Corrosion of X65 Steel Using Electrochemical Method, *International Journal of Electrochemical Science*, **10**, 10223 (2015). Doi: https://doi.org/10.1016/S1452-3981(23)11255-7
19. J. Idrac, G. Mankowski, G. Thompson, P. Skeldon, Y. Kihn, and C. Blanc, Galvanic corrosion of aluminium–copper model alloys, *Electrochimica Acta*, **52**, 7626 (2007). Doi: https://doi.org/10.1016/j.electacta.2007.05.056
20. X. Zhang, Q. Qian, L. Qiang, B. Zhang, and J. Zhang, Comparison study of gold coatings prepared by traditional and modified galvanic replacement deposition for corrosion prevention of copper, *Microelectronics Reliability*, **110**, 113695 (2020). Doi: https://doi.org/10.1016/j.microrel.2020.113695
21. D. Li, D. Botto, C. Xu, and M. Gola, Fretting wear of bolted joint interfaces, *Wear*, **458**, 203411 (2020). Doi: https://doi.org/10.1016/j.wear.2020.203411
22. P. Ojala, J. Rämö, J. Miettinen, and M. Vilkko, Reliability evaluation of CAN-bus connectors with tailored testing, *Mining Technology*, **132**, 203 (2023). Doi: https://doi.org/10.1080/25726668.2023.2235496